Rounding of Phase Transitions in Cylindrical Pores

Dorothea Wilms,[1] Alexander Winkler,[1] Peter Virnau,[1] and Kurt Binder[1]

[1]Institute of Physics, Johannes Gutenberg University Mainz,
Staudingerweg 7, D-55128 Mainz, Germany

Phase transitions of systems confined in long cylindrical pores (capillary condensation, wetting, crystallization, etc.) are intrinsically not sharply defined but rounded. The finite size of the cross section causes destruction of long range order along the pore axis by spontaneous nucleation of domain walls. This rounding is analyzed for two models (Ising/lattice gas and Asakura-Oosawa model for colloid-polymer mixtures) by Monte Carlo simulations and interpreted by a phenomenological theory. We show that characteristic differences between the behavior of pores of finite length and infinitely long pores occur. In pores of finite length a rounded transition occurs first, from phase coexistence between two states towards a multi-domain configuration. A second transition to the axially homogeneous phase follows near pore criticality.

Fluids and fluid mixtures in nano- and microporous materials (pore diameters from 1 nm to 150 nm) play important roles in various industries (extracting oil and gas from porous rocks; use as catalysts or for mixture separation in the chemical and pharmaceutical industry; nanofluidic devices, etc.) [1–3]. The interplay of finite size and surface effects strongly modifies the phase behavior of such confined fluids [1, 3–19] in comparison with the bulk. The vapor to liquid transition is shifted ("capillary condensation"), as well as critical points [3, 4, 9, 12]. Effects of wetting [20] on phase coexistence give rise to interesting patterns (plugs versus capsules versus tube structures etc. [7]). However, although various phase diagrams (different from the bulk) have been proposed (e.g. [1, 3, 7, 9, 12, 13, 17]), many aspects hitherto are not well understood. E.g., the "critical point" where adsorption/desorption hysteresis vanishes seems to be systematically lower than the critical temperature where the density difference between the vapor-like and liquid-like states vanishes [12], in contrast to what theories have predicted [14].

However, a crucial aspect (stressed only in a few pioneering studies [3, 8], and in the context of Ising/lattice gas models [21–23]) is the rounding of all transitions, caused by the quasi-one-dimensional character of a fluid in a long cylindrical pore with cross-sectional radius R. With the current progress of producing pores of well-controlled diameter varying from the nanoscale (carbon nanotubes [23–25]) to arrays of pores in silicon wafers [26], up to 150 nm wide and of well-controlled length, experiments become feasible which are not plagued by effects of random disorder, which occur in porous glasses [1, 27]. Thus, it is important to understand the phase transitions in pores more precisely, considering both the radius R and the length L of the pore as variables (the important role of L has so far been largely disregarded). In the present Letter, we elucidate the rounding of vapor-liquid type transitions in cylindrical pores, based on Monte Carlo simulations of two generic models and a phenomenological theory. We show that, even in the absence of precursors of wetting, two rounded transitions occur. Near the pore critical temperature at the pressure where vapor and liquid in the pore coexist, a rounded transition occurs from a axially homogenous state to a multi-domain configuration, where vapor-like and liquid-like domains alternate. The properties in this region depend strongly on R but not at all on L. In contrast, at lower temperatures the system makes a transition, where the full capillary is either in a vapor-like or a liquid-like state. The location of this transition depends on L, and the vapor to liquid transition is accompanied by a pronounced hysteresis. We also show that the effective (size-dependent) free energy exhibits well-defined spinodals (as a finite size effect), but they do not control dynamics. Nucleation of domain walls becomes dominant when their free energy cost are small (of order of a few $k_B T$, T being the temperature; henceforth $k_B = 1$). This domain wall nucleation explains why the hysteresis disappears far below the capillary critical region for small pores.

The simplest model that already shows some of these effects is the two-dimensional (2-d) Ising model on the square lattice in the geometry of $D \times L$ strips with periodic boundary conditions in both directions [21–23, 28]. While this 2-d model lacks the surface effects due to the walls of real 3-d pores, it exhibits already the disappearance of hysteresis far below pore criticality, since the condition $L >> D$ suffices to stabilize multi-domain states, as we will show below. Spins $S_i = \pm 1$ at lattice sites i interact with their nearest neighbors with an energy $J = 1$, and an external field H. We apply the standard single spin-flip Monte Carlo algorithm [29] and record the magnetization $M = \sum_{i=1}^{N} S_i / N$ ($N = LD$; the lattice spacing being the unit of length) as a function of H at various T. We start out with all spins up and $H = 0.05$. The system runs for a "time" $t = 2 \cdot 10^6$ Monte Carlo steps per spin (MCS). Then we decrease H

in steps of $\Delta H = 0.001$, and run the simulation at each field for the same time, until we reach $H = -0.05$. Afterwards, we reverse the process and increase the field stepwise by ΔH until we are back at $H = 0.05$. The width of the resulting hysteresis loops (Fig. 1a) strongly decreases with increasing T and for $T > T_0(L, D)$, the "hysteresis critical point", a hysteresis is no longer observed. However, when we record the probability distribution $P(M)$ for $H = 0$ with the Wolff cluster algorithm [29, 30] we observe that $P(M)$ still exhibits peaks very close to the (exactly known [31]) spontaneous magnetization M_s at temperatures $T > T_0(L, D)$. While for $L = 480$, $D = 10$ these peaks can be followed up to about $T = 2.1$, the peaks occur up to about the critical temperature for $D = 10$ and smaller L, e.g. $L = 40$. However, at $T_0(L, D)$ an important change also occurs in $P(M)$: while for $T < T_0(L, D)$ for a wide range of M $P(M)$ is strictly independent of M (corresponding to a slab configuration which contains exactly two non-interacting interfaces [32]), for $T > T_0(L, D)$ a third broad peak in $P(M)$ appears at $M = 0$. An examination of snapshot pictures of the system (Fig. 1b) reveals that this 3rd peak is due to multi-domain configurations [28, 33, 34].

Such multi-domain configurations can in fact be predicted when one computes the correlation length ξ along the strip (Fig. 2a) by transfer matrix methods (for $L \to \infty$ [22]) or Monte Carlo (for $L \gg \xi$ [33, 34]). The latter estimates were extracted from the wave vector-dependent susceptibility $\chi(\vec{k})$ for $\vec{k} = \vec{k}_{\min} = (2\pi/L, 0)$

$$\xi = \frac{1}{2\sin(k_{\min}/2)}\left[\frac{\chi(0)}{\chi(\vec{k}_{\min})} - 1\right]^{1/2} \quad , \quad (1)$$

and agree perfectly with the exact results. Thus, for very long strips the statistical errors are also well under control.

This correlation length below criticality (where well-defined domains exist) just measures the typical distance between domain walls along the strip. The approximation based on the (exactly known [35]) interfacial free energy σ, $\xi \approx \exp(D\sigma/T)$ becomes only accurate when $\xi \geq 10^5$, i.e. at temperatures much lower than those of interest for Fig. 1. This simply represents the well-known argument [36] that long-range order in quasi-one-dimensional systems is destroyed due to the entropy gain of putting interfaces into the system. The free energy difference (relative to the single-domain state) for a state with n (non-interacting) interfaces is $F = nF_{\text{int}} + nT\ln(n/eL)$, where the total free energy cost of one interface is given by $F_{\text{int}} = D\sigma$.

The occurrence of the central peak at T near $T_0(L, D)$ means that when T is raised at $H = 0$ there is a transition from nonzero $\langle|M|\rangle$ for $T < T_0(L, D)$ to a state with no order ($\langle|M|\rangle \ll M_s$) for $T > T_0(L, D)$. We characterize this transition by the weight of the central peak of $P(M)$, defined as $W = \int\limits_{-m}^{+m} P(M)dM / \int\limits_{-1}^{+1} P(M)dM$ where $\pm m$
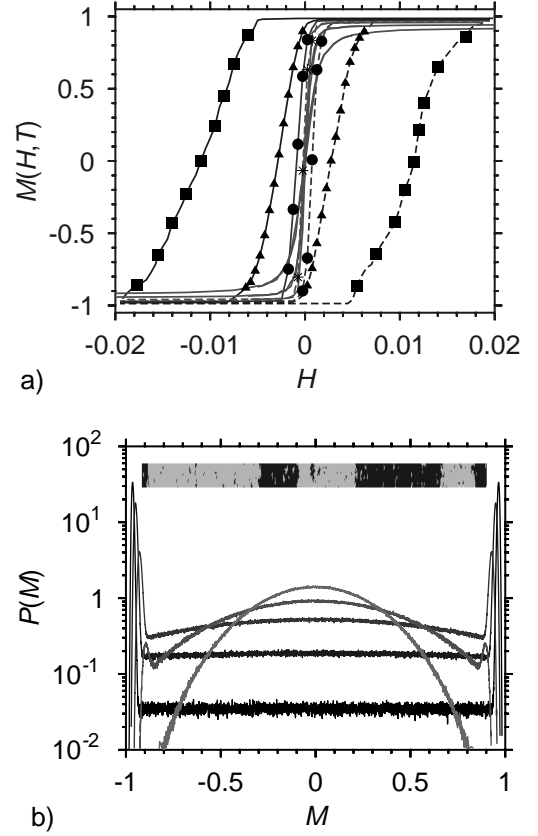

FIG. 1: (a) Magnetization of Ising strips for $L = 480$, $D = 10$ plotted vs. field H at $T = 1.5$■, 1.6▲, 1.7●, 1.8⋆, 1.9 and 2.0. Runs with decreasing H are shown as full curves, with increasing H as broken curves. A detailed analysis shows that the hysteresis disappears at $T_0 = 1.9$ in this case. (b) Distribution $P(M)$ vs. M for $H = 0$ and $T = 1.8 - 2.2$ from bottom to top at $M = 0$. The inset is a typical snapshot at $T = 2.1$ containing multiple domains stretched in y-direction by a factor ≈ 4.

are the locations of the minima of $P(M)$. Fig. 2 shows that the "equal weight" rule (first order transitions from one state to another state occur when the weights of the two states are $W = 1/2$) roughly corresponds to the condition $\xi \approx L/3$. With increasing L the transition gets shifted to lower temperature and also gets sharper. Since $W \approx 0.1$ for $\xi = L$ and $W \approx 0.9$ for $\xi = L/9$, we use $\xi \approx \exp(D\sigma/T) \approx \exp(2D/T)$ for low T for $L \to \infty$ to estimate both the location of the transition and its width ΔT,

$$T_0(L, D) \approx \frac{2D}{\ln(L/3)}, \quad L \to \infty, \quad \frac{\Delta T}{T_0(L, D)} \approx \frac{\ln 3}{\ln(L/9)} \quad (2)$$

Finally, defining a barrier ΔF from $P(M)$ as $\Delta F = T\ln[P(M_{\max})/P(m)]$ we see (Fig. 3a) why the transition at $T_0(L, D)$ is related to the vanishing of hysteresis: $\Delta F(T) \to 0$ at a temperature where $M_{\max}$ and m merge, which is close to $T_0 + \Delta T$ where $W \to 1$. Actually, the hysteresis already vanishes when $\Delta F/T \approx 10$ since then
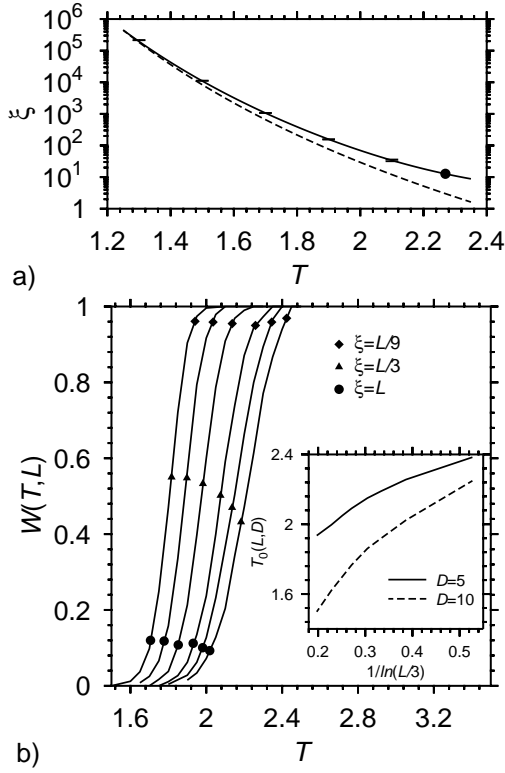
FIG. 2: (a) Correlation length ξ (on a logarithmic scale) plotted vs. T for Ising strips of width $D = 10$. Monte Carlo results (shown with error bars) were extracted for a system of $L = 10000$, recording the wavevector-dependent susceptibility $\chi(\vec{k}) = N\langle|M(\vec{k})|^2\rangle$ where $M(\vec{k}) = \sum S_j \exp(i\vec{k} \cdot \vec{r}_j)$ for $\vec{k}$ oriented in the long direction and $k = k_{\min} = 2\pi/L$, using the formula quoted in the text. Transfer matrix results were computed from the exact formula {Eq.(4.39)of [22]} for the $D \times \infty$ system. Broken curve shows the approximation $\xi \approx \exp(D\sigma/T)$ where σ is the exactly known interfacial tension of the Ising model. The value of ξ at T_c [21], $\xi_c = (4D/\pi)$, is shown as a dot. (b) Weight W of the central peak for strips of width $D = 10$ plotted vs. temperature for $L = 1000, 480, 240, 120, 80, 60$ from the left to the right. The symbols indicate $\xi = L, L/3$ and $L/9$, respectively. Insert shows a plot of $T_0(L,D)$ vs. L (note logarithmic scale) for two choices of D.

nucleation of interfaces is sufficiently easy.

In order to show that these results carry over to fluids confined in long cylindrical pores, we have studied the Asakura-Oosawa (AO) model [37] of colloid-polymer-mixtures. The latter system is attractive for experiments: the large colloid size renders effects of the atomistic corrugation of pore walls negligible, and facilitates observation of wetting layers and interfaces [38]. We describe colloids as hard spheres of radius $r_c = 1$, and polymers as soft spheres of radius $r_p = 0.8$. Polymer-colloid overlap (as well as colloid-colloid overlap) is strictly forbidden, while polymers can overlap with no energy cost. The phase diagram of this model in the bulk and for thin films has already been carefully studied [39, 40]. At the cylinder
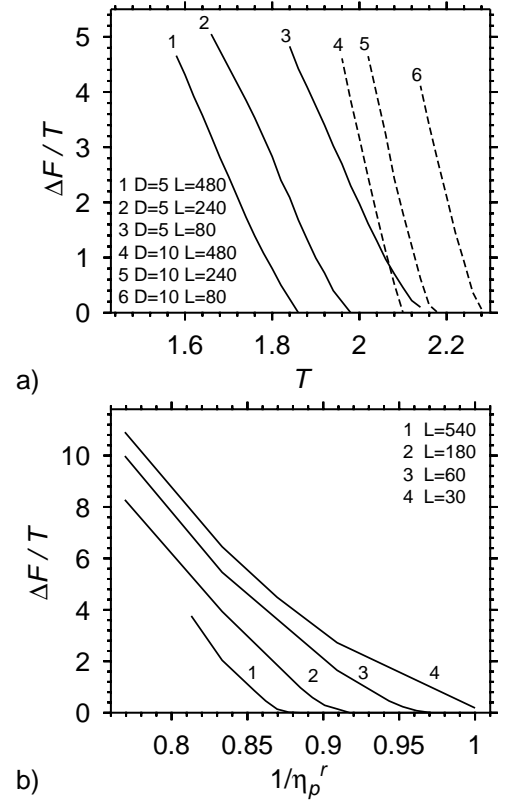

FIG. 3: (a) Barrier $\Delta F/T$ against nucleation of interfaces in Ising strips plotted vs. T. Several choices of L and D are shown, as indicated. (b) Barrier $\Delta F/T$ against nucleation of interfaces in the AO model confined to cylindrical pores of diameter $D = 12$ plotted vs. inverse polymer reservoir packing fraction $1/\eta_p^r$.

radius $R = D/2$ we apply a hard wall, which may overlap with neither colloids nor polymers. This boundary condition at the surface leads to an entropic attraction of the colloidal particles to the wall [40], causing the formation of a precursor of a wetting layer (a true wetting layer can only form in the limit $D \to \infty$, of course [40]).

For this model, the polymer fugacity $\exp(\mu_p/k_BT)$ or the related "polymer reservoir packing fraction" $\eta_p^r = (4\pi r_p^3/3)\exp(\mu_p/k_BT)$ plays the role of an inverse temperature like variable, while the colloid packing fraction $\eta_c = (4\pi r_c^3/3)N_c/V$ (N_c is the number of colloids in the system of volume $V = \pi R^2 L$) is the order parameter density. Fig. 4(a), as a counterpart of Fig. 1(b), shows $P(\eta_c)$ for various values of η_p^r. (The same Grand Canonical Monte Carlo methods as in [39] are used.) One can clearly distinguish the crossover from an (asymmetric) double-peak distribution to a structure with three peaks, and finally a single peak, which only narrows when η_p^r is close to $\eta_{p,crit}^r = 0.766$ [39]. The "phase diagram", where the coexisting polymer-rich and colloid-rich phases are estimated from the left-most to the right-most peak in Fig. 4(a), is shown in Fig. 4(b). Fig. 3(b) shows that the barrier against nucleation of interfaces across the
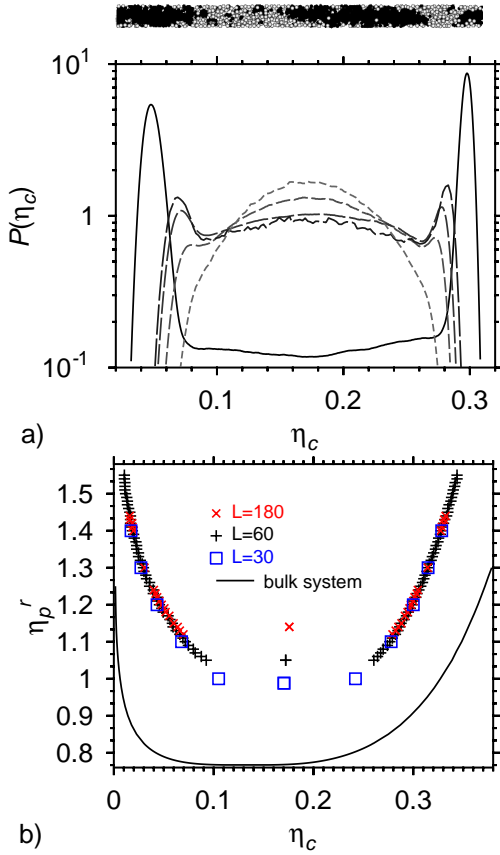
FIG. 4: (a) Distribution $P(\eta_c)$ of the number of colloids in a cylinder of diameter $D = 12$ and length $L = 180$ (all lengths are measured in units of the colloid radius) for $\eta_p^r = 1.075, 1.10, 1.115, 1.118, 1.20$ from top to bottom at $\langle \eta_c \rangle \approx 0.175$. Above the plot we show a typical snapshot (cross section through the cylinder) at $\eta_p^r = 1.10$ containing multiple domains. (b) Phase diagram of the AO model in a cylindrical pore of diameter $D = 12$ and lengths $L = 30$, 60 and 180, as indicated. The full curve is the bulk coexistence curve [39]. Note that the points shown near $\langle \eta_c \rangle \approx 0.16$ to 0.17 mark $\eta_{p0}^r(D, L)$ for three choices of L.

pore strongly decreases with increasing L, and we have checked [34] that hysteresis disappears when the barrier is a few $k_B T$, as for the Ising model.

In summary, we have clarified the nature of phase coexistence between vapor and liquid phases of fluids (or fluid-fluid phase coexistence of mixtures) in long cylindrical pores, depending on pore length L and pore diameter D. While at high temperatures the structure of the fluid is axially symmetric, phase separation in axial direction sets in at the coexistence pressure when the correlation length (of the density fluctuations) ξ grows to the order of D. Below the pore critical temperature ξ measures the distance between domain walls, and at a much lower temperature (where $\xi \approx L/3$) a second (again rounded) transition occurs (the pore then is either in an axially homogeneous vapor-like or liquid-like state). The

onset of adsorption hysteresis in the capillary is linked to this lower transition. A wetting transition (possible at a flat surface of a semi-infinite system) is also expected to be strongly rounded in narrow pores, and should not change the above conclusions. Our findings provide insight to understand experiments and simulations of fluids in pores, explaining the existence of a "hysteresis critical point" distinct from the pore critical point. A prediction that experiments could test is the decrease of the hysteresis critical temperature with increasing pore length.

[1] L.D. Gelb et al., Rep. Progr. Phys. **62**, 1573 (1999)
[2] T. Thorsen et al., Science **298**, 580 (2002)
[3] I. Brovchenko and A. Oleinikova, *Interface and Confined Water* (Elsevier, Amsterdam, 2008)
[4] R. Evans et al., J. Chem. Soc. Faraday Trans **2**, 1763 (1986)
[5] G. Heffelfinger et al., Mol. Phys. **60**, 1381 (1987)
[6] R. Evans, J. Phys.: Condens. Matter **46**, 9899 (1990)
[7] A.J. Liu et al., Phys. Rev. Lett. **65**, 1897 (1990)
[8] L.D. Gelb and K.E. Gubbins, Phys. Rev. E**56**, 3185 (1997)
[9] K. Morishige et al., Langmuir **13**, 3494 (1997)
[10] P.L. Ravikovich et al., J. Phys. Chem. B**101**, 3671 (1997)
[11] A.V. Neimark et al., J. Colloid Interface Sci. **207**, 159 (1998)
[12] K. Morishige and M. Shikimi, J. Chem. Phys. **108**, 7821 (1998)
[13] W.D. Machin, Langmuir **15**, 169 (1999)
[14] A. Vishnyakov and A.V. Neimark, J. Phys. Chem. B**105**, 7009 (2001)
[15] H.K. Christenson, J. Phys.: Condens. Matter **13**, R95 (2001)
[16] A. Schreiber et al., Mol. Phys. **100**, 2097 (2002); K.G. Kornev et al., Adv. Coll. Interface Sci. **96**, 143 (2002)
[17] J. Hoffmann and P. Nielaba, Phys. Rev. E**67**, 036115 (2003)
[18] C. Alba-Simionesco et al. J. Phys.: Condens. Matter **18**, R15 (2006)
[19] I. Brovchenko, A. Geiger, and A. Oleinikova, J. Phys. Condens. Matter **16**, S5345 (2007)
[20] S. Dietrich, in *Phase Transitions and Critical Phenomena*, edited by C. Domb and J.L. Lebowitz (Academic, London, 1988) Vol 12, Chap. 1
[21] V. Privman and M.E. Fisher, J. Stat. Phys. **33**, 385 (1983)
[22] M.N. Barber, in *Phase Transition and Critical Phenomena* edited by C. Domb and J.L. Lebowitz (Academic, London, 1983) Vol 8, Chap. 2.
[23] P. Nowakowski and M. Napiorkowski, J. Phys. A: Math. Theor. **42**, 475005 (2009)
[24] S. Inoue et al., J. Phys. Chem. B**102**, 4689 (1998)
[25] M. Meyyappan (ed.) *Carbon Nanotubes: Science and Applications* (CRC Press, Boca Raton, 2004)

[26] Z.N. Yu et al., J. Vac. Sci. Technol. B**21**, 2874 (2003)

[27] P. Wiltzius et al., Phys. Rev. Lett. **62**, 804 (1989); M.Y. Lin et al., Phys. Rev. Lett. **72**, 2207 (1994)

[28] E.V. Albano et al., Z. Phys. B: Condens. Matter **77**, 445 (1989)

[29] D.P. Landau and K. Binder, *A Guide to Monte Carlo Simulation in Statistical Physics, 3rd ed.* (Cambridge Univ. Press, Cambridge, 2009)

[30] U. Wolff, Phys. Rev. Lett. **62**, 361 (1989)

[31] C.N. Yang, Phys. Rev. **85**, 808 (1952)

[32] K. Binder, Phys. Rev. A**25**, 1699 (1982)

[33] D. Wilms, Diplomarbeit, Johannes Gutenberg Univ. Mainz (2009, unpublished)

[34] More details will be presented in a forthcoming full paper (A. Winkler et al., unpublished)

[35] L. Onsager, Phys. Rev. **65**, 117 (1944)

[36] L.D. Landau and E.M. Lifshitz, *Statistical Physics, 3rd ed.* (Pergamon Press, Oxford, 1959)

[37] S. Asakura and F. Oosawa, J. Chem. Phys. **22**, 1255 (1957)

[38] Y. Hennequin et al., Phys. Rev. Lett. **100**, 178305 (2008)

[39] R.L.C. Vink and J. Horbach, J. Chem. Phys. **121**, 3253 (2004)

[40] K. Binder et al., Soft Matter **4**, 1555 (2008)